

## Equivalent linearization technique in non-linear stochastic dynamics of a cable-mass system with time-varying length

H. WEBER<sup>1)</sup>, R. IWANKIEWICZ<sup>1,2)</sup>, S. KACZMARCZYK<sup>3)</sup>

<sup>1)</sup>*West Pomeranian University of Technology, Szczecin, Poland,  
e-mail: Hanna.Weber@zut.edu.pl*

<sup>2)</sup>*Institute of Mechanics and Ocean Engineering, Hamburg University of Technology,  
Germany, e-mail: iwankiewicz@tu-harburg.de*

<sup>3)</sup>*Faculty of Arts, Science and Technology, University of Northampton,  
The United Kingdom, e-mail: Stefan.Kaczmarczyk@northampton.ac.uk*

IN THIS PAPER THE TRANSVERSE VIBRATIONS OF A VERTICAL CABLE carrying a concentrated mass at its lower end and moving slowly vertically within the host structure are considered. It is assumed that longitudinal inertia of the cable can be neglected, with the longitudinal motion of the concentrated mass coupled with the lateral motion of the cable. An expansion of the lateral displacement of a cable in terms of approximating functions is used. The excitation acting upon the cable-mass system is a base-motion excitation due to the sway motion of a host tall structure. Such a motion of a structure often results due to action of the wind, hence it may be adequately idealized as a narrow-band random process. The narrow-band process is represented as the output of a system of two linear filters to the input in a form of a Gaussian white noise process. The non-linear problem is dealt with by an equivalent linearization technique, where the original non-linear system is replaced with an equivalent linear one, whose coefficients are determined from the condition of minimization of a mean-square error between the non-linear and the linear systems. The mean value and variance of the transverse displacement of the cable as well as those of the longitudinal motion of the lumped mass are determined with the aid of an equivalent linear system and compared with the response of the original non-linear system subjected to the deterministic harmonic excitation.

**Key words:** cable-mass system, stochastic dynamics, equivalent linearization technique.

Copyright © 2019 by IPPT PAN, Warszawa

### 1. Introduction

AXIALLY MOVING ELASTIC STRINGS, BELTS, ROPES AND CABLES carrying inertia elements such as rigid-body masses are important elements of many engineering systems. In many applications the length of hoisting cables and ropes vary when the system is in operation, for example due to the transport motion applied to carry the payload (mass), which results in non-stationary behaviour

of the system. Also traction drive elevators employ ropes of variable length as a means of car suspension and for the compensation of tensile forces over the traction sheave. Other applications are travelling cables used to transmit power and communication signals between the elevator car and control unit [1] or ropes and cables employed as important structural elements of offshore and marine towing installations. Tethers experiencing extension and retraction deployed in a variety of different space vehicle propulsion systems based on applications of momentum exchange and electrodynamic interactions with planetary magnetic fields are also examples of such systems [2]. Apart from the transport longitudinal motion those slender continua are subject to various excitation sources and experience longitudinal vibrations. The longitudinal vibrations are coupled with transverse vibrations which is one of the reasons for the non-linear behaviour of such systems. Phenomena such as passage through resonance [3] and non-linear modal interactions often arise.

In this paper a system comprising a rigid mass suspended on an elastic cable in a tall slender structure is considered. Environmental phenomena such as strong wind conditions and/or earthquakes cause tall slender civil engineering structures such as towers and high-rise buildings to vibrate (sway) at low frequencies and large amplitudes [4, 5]. As a result, cables and ropes that are part of equipment hosted within the structure are being excited. For example, large resonance motions of suspension ropes and compensating cables in high-speed elevators in high-rise buildings take place [6]. In order to predict the dynamic behavior of such systems the excitation mechanism can be represented by deterministic functions and consequently the response of the system has been treated as a deterministic phenomenon. However, the nature of loading caused by wind is usually nondeterministic [7–10]. Action of the wind may be regarded as a wide-band random process. Consequently, the dynamic response of a structure, which is a lightly damped linear dynamic system, is a narrow-band random process. It is a base-motion type excitation to the hoisting ropes hosted within the structure.

Due to the non-stationary and non-linear nature of the problem solving the non-stationary non-linear deterministic/stochastic equations describing the system behaviour by applying analytical methods is difficult [11]. Perturbation methods can be used [12] but the most convenient approach is to apply direct numerical techniques. A similar problem was dealt with in [13]. In that paper an approximate linear model was developed by neglecting non-linear terms in the equations of motion. In the present paper an equivalent (statistical) linearization technique is used. The essence of this technique is the replacement of the original non-linear system with an equivalent linear system, whose coefficients are determined from the condition of mean-square minimization of the error between the linear system and the non-linear one. These coefficients are expressed in terms of expectations of non-linear functions (e.g. moments) of the response process (state

variables). In problems of random vibrations induced by Gaussian excitations these expectations are evaluated with the aid of the Gaussian probability density function assumed as the tentative density. This is so, because the response of a linear system to a Gaussian excitation is also Gaussian. The statistical linearization technique was first used for problems of non-linear random vibrations by CAUGHEY [14]. This technique has ever since found applications to a great variety of non-linear stochastic problems in structural dynamics. The statistical linearization technique together with its different applications is covered e.g. in [15–18]. It is worthwhile to note that the equivalent linearization technique was also applied to the problems of non-Gaussian excitations. In [19] a non-linear system under a Poisson impulse excitation was considered. As the non-linearity was of cubic form, the necessary expectations were just higher-order moments, which were assumed as response moments of a linear system (filtered Poisson process). A similar approach was used in [20]. Another version of equivalent linearization technique was developed in [21] for the non-linear hysteretic system under Poisson-distributed pulse trains. The tentative probability density function required for the evaluation of expectations of non-polynomial non-linear functions was assumed in a non-Gaussian form of a truncated Gram–Charlier expansion. More recently statistical linearization technique has been applied in combination with different advanced methods of stochastic dynamics, e.g. [22–25].

In this paper the mean value and variance of the transverse displacement of the cable as well as those of a longitudinal motion of the lumped mass are determined with the aid of an equivalent linear system and compared with the response of the original non-linear system subjected to the deterministic harmonic excitation and results from the Monte Carlo simulation.

## 2. Non-linear system

In this section the cable-mass system with time-varying length is considered from the point of view of the non-linear deterministic solution. Figure 1a illustrates a lift installation, mounted in a lift shaft within a tall building structure. The external dynamic loads lead to excitation of structural parts, such as cables and ropes, of the lift system. Let us consider a schematic model of a cable-mass system mounted with the host structure, that is presented in Fig. 1b.

The concentrated mass  $M$  is attached to the lower end of a vertical elastic cable and moves slowly axially with the transport speed  $V$  and acceleration/deceleration  $a$ . Therefore, the length of the cable in lifting installations varies over time  $L = L(t)$ . The characteristics of the cable such as mass per unit length, modulus of elasticity and cross-sectional metallic area are denoted as  $m$ ,  $E$  and  $A$ , respectively. The longitudinal vibrations of the mass are assumed as  $u_M$  while the lateral displacements at the top of the host structure as  $v_0$ . The

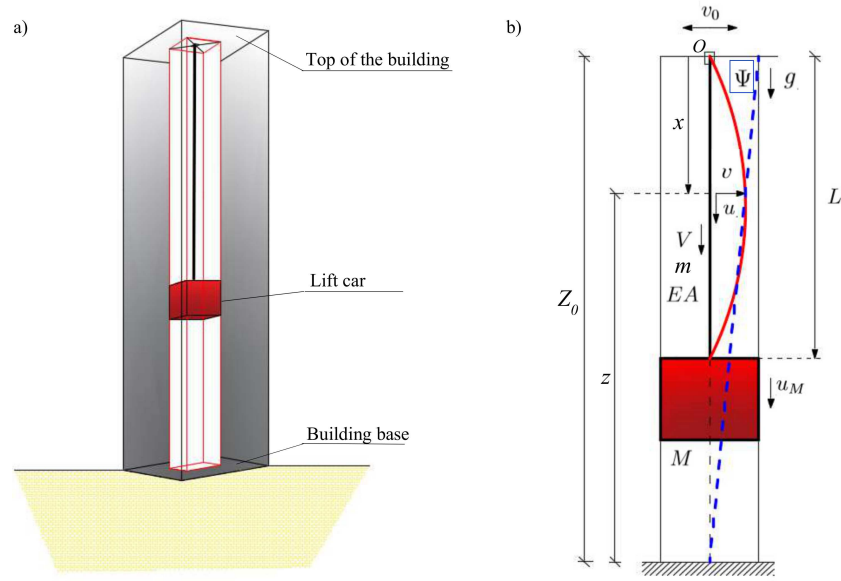


FIG. 1. a) High-rise building with lift installation; b) lift car-cable system schematic model.

cable longitudinal vibrations  $u(x, t)$  considered at chosen level  $x$ , are coupled with its lateral displacements  $v(x, t)$ .

In this case the cable strain measure is assumed as  $\varepsilon = u_x + \frac{1}{2}v_x^2$  and the quasi-static tension of the cable is given by the expression  $T = (M + mL)(g - a)$ . Hamilton's Principle accounting for the external work of non-conservative forces, kinetic and potential energies of the system is used to derive the equations of motion of the system. Then the following partial differential equations of motion are obtained

$$(2.1) \quad \begin{aligned} m \frac{d^2 u}{dt^2} - EA \varepsilon_x &= 0, \\ m \frac{d^2 v}{dt^2} - T v_{xx} + m(g - a)(x v_{xx} + v_x) - EA(\varepsilon v_x)_x &= 0, \\ M \ddot{u}_M + EA \varepsilon|_{x=L} &= 0. \end{aligned}$$

where the total derivative is given by the equation

$$(2.2) \quad \frac{d^2(\cdot)}{dt^2} = (\cdot)_{tt} + 2V(\cdot)_{xt} + V^2(\cdot)_{xx} + a(\cdot)_x.$$

The last equation in (2.1) determines the boundary condition for the longitudinal motion at  $x = L$  with  $u_M = u(L, t)$ . Since for tensioned metallic ropes and cables the lateral natural frequencies are much lower than the longitudinal

natural frequencies and the lateral excitations frequencies are much lower than the fundamental longitudinal frequencies, the longitudinal inertia of the cable presented in the first equation in (2.1) can be neglected. Integrating this equation and using boundary conditions  $u(0, t) = 0$  and  $u(L, t) = u_M(t)$  yields to the following expression

$$(2.3) \quad u_x + \frac{1}{2}v_x^2 = e(t), \quad e(t) = \frac{u_M}{L} + \frac{1}{2L} \int_0^L v_x^2 dx.$$

Using (2.2) and (2.3) in (2.1) gives the following set of two equations

$$(2.4) \quad \begin{aligned} mv_{tt} - \left\{ T + m \left[ (a - g)x - V^2 \right] + \frac{EA}{L} \left( u_M + \frac{1}{2L} \int_0^L v_x^2 dx \right) \right\} v_{xx} \\ + mgv_x + 2mVv_{xt} = 0, \\ M\ddot{u}_M + \frac{EA}{L} \left( u_M + \frac{1}{2L} \int_0^L v_x^2 dx \right) = 0. \end{aligned}$$

The sway of the structure causes the bending deformations of the host structure that can be described approximately by the polynomial shape function

$$\Psi(\eta) = 3\eta^2 + 2\eta^3,$$

where the variable  $\eta = \frac{z}{Z_0}$  is the ratio of  $z$  coordinate measured from the ground level and height  $Z_0$  of the entire system. The bending deformations produce harmonic motion  $v_0(t)$  with the amplitude  $A_0$  and frequency  $\Omega_0$  at the top end of the cable. The time dependent lateral displacements at the lower end of the cable can be expressed by the equation

$$(2.5) \quad v_L(t) = \Psi_L v_0(t),$$

where the  $\Psi_L$  is given in the form

$$(2.6) \quad \Psi_L = \Psi \left( \frac{Z_0 - L(t)}{Z_0} \right).$$

It can be assumed that the change of  $L(t)$  over a period  $T_0$  corresponding to the fundamental frequency of the system (denoted as  $f_0$ ) is small in comparison with the total length of the cable [3,12], the slow time scale is defined as  $\tau = \epsilon t$ . The small parameter  $\epsilon \ll 1$  is defined by the equation  $\epsilon = \dot{L}(t_0)/f_0 L_0$  [13], with  $t_0$  being the given time instant corresponding to  $f_0$  and  $L_0 = L(t_0)$ . Assuming

$L = L(\tau)$ , in order to accommodate the base excitation, the relative lateral displacements can be expressed by the following truncated series in the form as

$$(2.7) \quad v(x, t, \tau) = \bar{v}(x, t; \tau) + \bar{V}_0(x, t) \\ = \sum_{n=1}^N \Phi_n[x, L(\tau)] q_n(t) + \left(1 + \frac{\Psi_1 - 1}{L} x\right) v_0(t),$$

where orthogonal trial functions are defined as  $\Phi_n[x, L(\tau)] = \sin \frac{n\pi}{L(\tau)} x$ ,  $n = 1, \dots, N$  with  $N$  denoting the number of modes taken into consideration. When the expansion of the displacements  $v(x, t)$  in terms of approximating functions is used, the following set of differential equations of motion is obtained as [13]

$$(2.8) \quad \ddot{q}_r(t) + 2\zeta_r \omega_r(\tau) \dot{q}_r(t) + \sum_{n=1}^N C_{rn}(\tau) \dot{q}_n(t) + \sum_{n=1}^N K_{rn}(\tau) q_n(t) \\ + \lambda_r^2(\tau) c^2 q_r(t) \sum_{n=1}^N \beta_n^2(\tau) q_n^2(t) \\ + \lambda_r^2 \left\{ \bar{c}^2 - V^2 + c^2 \left[ \frac{u_M(t)}{L(\tau)} + \frac{1}{2} \left( \frac{\Psi_L - 1}{L(\tau)} \right)^2 v_0^2(t) \right] \right\} q_r(t) \\ = Q_r(t, \tau); \quad r = 1, \dots, N, \\ \ddot{u}_M(t) + 2\zeta_M \omega_M(\tau) \dot{u}_M(t) + \omega_M^2(\tau) u_M + \frac{EA}{M} \sum_{n=1}^N \beta_n^2(\tau) q_n^2(t) \\ = -\frac{EA}{2M} \left( \frac{\Psi_L - 1}{L(\tau)} \right)^2 v_0^2(t).$$

In Eqs. (2.8)  $\zeta_r$ ,  $\zeta_M$  are the modal damping ratios,  $\omega_M$  and  $\omega_r$  denote undamped natural frequencies of the system, while  $q_r(t)$  are the generalized coordinates corresponding to the lateral modes which vary fast over time  $t$ . Other constants and variables used in the presented set of differential equations can be defined by the following expressions

$$\lambda_r(\tau) = \frac{r\pi}{L(\tau)}, \quad \beta_r(\tau) = \frac{1}{2} \lambda_r(\tau), \quad c = \sqrt{\frac{EA}{m}} \quad \text{and} \quad \bar{c} = \sqrt{\frac{T}{m}}.$$

It is assumed that the stiffness  $K_{rn}(\tau)$  and damping  $C_{rn}(\tau)$  coefficients vary slowly over time. Together with the modal excitation functions  $Q_r(t, \tau)$ , they

can be expressed by using the following equations [13]:

$$(2.9) \quad K_{rn}(\tau) = \begin{cases} \frac{L(\tau)}{2}(a-g)\lambda_r^2, & n = r, \\ \frac{2}{L(\tau)} \left[ g \frac{nr}{n^2 - r^2} + (a-g) \frac{2rn^3}{(n^2 - r^2)^2} \right] [(-1)^{r+n} - 1], & n \neq r, \end{cases}$$

$$C_{rn}(\tau) = \frac{4V}{L(\tau)} \begin{cases} 0, & n = r, \\ \frac{nr}{n^2 - r^2} [(-1)^{r+n} - 1], & n \neq r, \end{cases}$$

$$Q_r(t, \tau) = \frac{2}{r\pi} \left\{ [(-1)^r \Psi_L - 1] \ddot{v}_0(t) + \frac{\Psi_L - 1}{L(\tau)} [g v_0(t) + 2V \dot{v}_0(t)] [(-1)^r - 1] \right\}.$$

In the deterministic solution the displacement  $v_0(t)$  is assumed to be in the form of a harmonic motion related to the fundamental mode of the structure. Using Eqs. (2.8) and (2.9) an approximated single-mode model describing the behaviour of the system in the resonance region [13] can be obtained in the form

$$(2.10) \quad \ddot{q}_r(t) + 2\zeta_r \omega_r(\tau) \dot{q}_r(t) + \frac{L(\tau)}{2}(a-g)\lambda_r^2 q_r(t) + \frac{\lambda_r^4}{4} c^2(\tau) q_r^3(t) + \lambda_r^2 \left\{ \bar{c}^2 - V^2 + c^2 \left[ \frac{u_M(t)}{L(\tau)} + \frac{1}{2} \left( \frac{\Psi_L - 1}{L(\tau)} \right)^2 v_0^2(t) \right] \right\} q_r(t) = Q_1(t, \tau),$$

$$\begin{aligned} \ddot{u}_M(t) + 2\zeta_M \omega_M(\tau) \dot{u}_M(t) + \omega_M^2(\tau) u_M(t) + \frac{EA}{M} \frac{\lambda_r^2(\tau)}{4} q_r^2(t) \\ = -\frac{EA}{2M} \left( \frac{\Psi_L - 1}{L(\tau)} \right)^2 v_0^2(t). \end{aligned}$$

In the paper [13] the linearized problem was considered by neglecting the non-linear terms. In presented analysis the equivalent linearization technique is adopted to replace the original system governed by non-linear differential equations (2.10) with an equivalent system governed by linear differential equations.

### 3. Stochastic equations of motion

Due to the nature of the excitation caused by the excitation sources, for example, the external wind load, the motion  $v_0(t)$  can be considered as the narrow-band random process. For the sake of comparison this process is assumed to be mean-square equivalent to the deterministic harmonic process with the

amplitude  $A_0$  and frequency  $\Omega_0$ . The structural displacement response  $v_0(t)$  must be continuous and twice differentiable. These requirements can be satisfied by assuming  $v_0(t)$  as the response of the second order auxiliary filter to the process  $X(t)$ , which is the response of the first-order filter to the Gaussian white noise  $\xi(t)$  excitation [7]. The governing equations are adopted in the form

$$(3.1) \quad \begin{aligned} \ddot{v}_0(t) + 2\zeta_f \Omega_0 \dot{v}_0(t) + \Omega_0^2 v_0(t) &= X(t), \\ \dot{X}(t) + \alpha X(t) &= \alpha \sqrt{2\pi S_0} \xi(t), \end{aligned}$$

with  $\zeta_f$ ,  $S_0$  and  $\alpha$  being the damping ratio of the auxiliary filter, the level of the white noise power spectrum and the filter variable, respectively. The latter is expressed by the equation

$$(3.2) \quad \alpha = \Omega_0 \left( -\zeta_f + \sqrt{\zeta_f^2 + \frac{\zeta_f \Omega_0^3 A_0^2}{\pi S_0 - \zeta_f \Omega_0^3 A_0^2}} \right),$$

which assures satisfying the following expression

$$(3.3) \quad \text{Var}(v_0) = \sigma_{v_0}^2 = \frac{A_0^2}{2},$$

which in turn causes the stochastic process  $v_0(t)$  to be mean-square equivalent to the deterministic harmonic one. Second-order differential equations of motion are converted into first-order stochastic differential equations

$$(3.4) \quad d\mathbf{Y}(t) = \mathbf{c}(\mathbf{Y}(t), t)dt + \mathbf{d}(t)dW(t),$$

where  $W(t)$  denotes the standard Wiener process while  $\mathbf{c}(\mathbf{Y}(t), t)$  and  $\mathbf{d}(t)$  are the drift vector and the diffusion vector, respectively.  $\mathbf{Y}(t)$  is the augmented state vector assumed in the form

$$(3.5) \quad \mathbf{Y}(t) = [q_r(t) \quad \dot{q}_r(t) \quad u_M(t) \quad \dot{u}_M(t) \quad v_0(t) \quad \dot{v}_0(t) \quad X(t)]^T,$$

and the components of the drift vector are given by the equations

$$(3.6) \quad \begin{aligned} c_1(\mathbf{Y}(t)) &= \dot{q}_r(t), \\ c_2(\mathbf{Y}(t)) &= -C_r(\tau)\dot{q}_r(t) - K_r(\tau)q_r(t) \\ &\quad - c^2 \lambda_r^2 \left[ \frac{u_M(t)}{L(\tau)} + \frac{1}{2} \left( \frac{\Psi_L - 1}{L(\tau)} \right)^2 v_0^2(t) + \frac{\lambda_r^2}{4}(\tau)q_r^2(t) \right] q_r(t) \\ &\quad + (\beta_r^{(0)} - \beta_r^{(2)}\Omega_0^2)v_0(t) + (\beta_r^{(1)} - 2\beta_r^{(2)}\zeta_f\Omega_0)\dot{v}_0(t) + \beta_r^{(2)}X(t), \\ c_3(\mathbf{Y}(t)) &= \dot{u}_M(t), \end{aligned}$$

$$\begin{aligned}
c_4(\mathbf{Y}(t)) &= -2\zeta_M \omega_M(\tau) \dot{u}_M(t) - \omega_M^2(\tau) u_M(t) \\
&\quad - \frac{EA \lambda_r^2(\tau)}{M} \frac{q_r^2(t)}{4} - \frac{EA}{2M} \left( \frac{\Psi_L - 1}{L(\tau)} \right)^2 v_0^2(t), \\
(3.6)_{[\text{cont.}]} \quad c_5(\mathbf{Y}(t)) &= \dot{v}_0(t), \\
c_6(\mathbf{Y}(t)) &= X(t) - 2\zeta_f \Omega_0 \dot{v}_0(t) - \Omega_0^2 v_0(t), \\
c_7(\mathbf{Y}(t)) &= -\alpha X(t),
\end{aligned}$$

where the following expressions defining the coefficients  $\beta_r^{(0)}$ ,  $\beta_r^{(1)}$ ,  $\beta_r^{(2)}$  are adopted

$$\begin{aligned}
\beta_r^{(0)} &= \frac{2g}{\pi r} [(-1)^r - 1] \frac{\Psi_L - 1}{L(\tau)} \\
\beta_r^{(1)} &= \frac{4V}{\pi r} [(-1)^r - 1] \frac{\Psi_L - 1}{L(\tau)}; \\
\beta_r^{(2)} &= \frac{2}{\pi r} [(-1)^r \Psi_L - 1].
\end{aligned}$$

#### 4. Application of equivalent linearization technique

To use the equivalent linearization technique, the augmented state vector must be converted into the centralized state vector

$$(4.1) \quad \mathbf{Y}^0(\mathbf{t}) = [Y_1^0(t) \ Y_2^0(t) \ Y_3^0(t) \ Y_4^0(t) \ Y_5^0(t) \ Y_6^0(t) \ Y_7^0(t)]^T,$$

where

$$\begin{aligned}
(4.2) \quad Y_1^0(t) &= q_r(t) - \mu_{q_r}, \\
Y_2^0(t) &= \dot{q}_r(t) - \mu_{\dot{q}_r}, \\
Y_3^0(t) &= u_M(t) - \mu_{u_M}, \\
Y_4^0(t) &= \dot{u}_M(t) - \mu_{\dot{u}_M}, \\
Y_5^0(t) &= v_0(t) - \mu_{v_0}, \\
Y_6^0(t) &= \dot{v}_0(t) - \mu_{\dot{v}_0}, \\
Y_7^0(t) &= X(t) - \mu_X.
\end{aligned}$$

The differential equations for mean values are

$$(4.3) \quad \frac{d}{dt} \mu(t) = \mathbf{E}[\mathbf{c}(\mathbf{Y}^0(t))],$$

where

$$(4.4) \quad \mu(t) = [\mu_{q_r}, \mu_{\dot{q}_r}, \mu_{u_M}, \mu_{\dot{u}_M}, \mu_{v_0}, \mu_{\dot{v}_0}, \mu_X]^T,$$

By using Eqs. (3.6) and (4.2) the mean values from Eq. (4.3) are expressed as

$$\begin{aligned}
\mathbb{E}[c(\mathbf{Y}_1^0(t))] &= \mathbb{E}[Y_2^0(t) + \mu_{\dot{q}_r}], \\
\mathbb{E}[c(\mathbf{Y}_2^0(t))] &= \mathbb{E} \left[ -C_r(\tau)(Y_2^0(t) + \mu_{\dot{q}_r}) - K_r(\tau)(Y_1^0(t) + \mu_{q_r}) \right. \\
&\quad - \frac{c^2 \lambda_r^2}{L(\tau)} (Y_3^0(t) Y_1^0(t) + Y_1^0(t) \mu_{u_M} + Y_3^0(t) \mu_{q_r} + \mu_{u_M} \mu_{q_r}) \\
&\quad - \frac{c^2 \lambda_r^2}{2} \left( \frac{\Psi_L - 1}{L(\tau)} \right)^2 ((Y_5^0(t))^2 Y_1^0(t) + (Y_5^0(t))^2 \mu_{q_r}) \\
&\quad - \frac{c^2 \lambda_r^2}{2} \left( \frac{\Psi_L - 1}{L(\tau)} \right)^2 (2Y_5^0(t) Y_1^0(t) \mu_{v_0}) + 2Y_5^0(t) \mu_{v_0} \mu_{q_r} + Y_1^0(t) \mu_{v_0}^2 \\
&\quad - \frac{c^2 \lambda_r^2}{2} \left( \frac{\Psi_L - 1}{L(\tau)} \right)^2 \mu_{v_0}^2 \mu_{q_r} + (\beta_r^{(0)} - \beta_r^{(2)} \Omega_0^2) (Y_5^0(t) + \mu_{v_0}) \\
(4.5) \quad &\quad - \frac{c^2 \lambda_r^4}{4} (\tau) ((Y_1^0(t))^3 + 3(Y_1^0(t))^2 \mu_{q_r} + 3Y_1^0(t) \mu_{q_r}^2 + \mu_{q_r}^3) \\
&\quad \left. + (\beta_r^{(1)} - 2\beta_r^{(2)} \zeta_f \Omega_0) (Y_6^0(t) + \mu_{\dot{v}_0}) + \beta_r^{(2)} (Y_7^0(t) + \mu_X) \right], \\
\mathbb{E}[c(\mathbf{Y}_3^0(t))] &= \mathbb{E}[Y_4^0(t) + \mu_{\dot{u}_M}], \\
\mathbb{E}[c(\mathbf{Y}_4^0(t))] &= \mathbb{E} \left[ -2\zeta_M \omega_M(\tau) (Y_4^0(t) + \mu_{\dot{u}_M}) - \omega_M^2(\tau) (Y_3^0(t) + \mu_{u_M}) \right. \\
&\quad - \frac{EA}{M} \frac{\lambda_r^2(\tau)}{4} ((Y_1^0(t))^2 + 2Y_1^0(t) \mu_{q_r} + \mu_{q_r}^2) \\
&\quad \left. - \frac{EA}{2M} \left( \frac{\Psi_L - 1}{L(\tau)} \right)^2 ((Y_5^0(t))^2 + 2Y_5^0(t) \mu_{v_0} + \mu_{v_0}^2) \right], \\
\mathbb{E}[c(\mathbf{Y}_5^0(t))] &= \mathbb{E}[Y_6^0(t) + \mu_{\dot{v}_0}], \\
\mathbb{E}[c(\mathbf{Y}_6^0(t))] &= \mathbb{E}[Y_7^0(t) + \mu_X - 2\zeta_f \Omega_0 (Y_6^0(t) + \mu_{\dot{v}_0}) - \Omega_0^2 (Y_5^0(t) + \mu_{v_0})], \\
\mathbb{E}[c(\mathbf{Y}_7^0(t))] &= \mathbb{E}[-\alpha (Y_7^0(t) + \mu_X)].
\end{aligned}$$

The stochastic equations for the centralized state vector are obtained as

$$(4.6) \quad d\mathbf{Y}^0(t) = \mathbf{c}^0(\mathbf{Y}^0(t), t) dt + \mathbf{d}(t) dW(t).$$

The centralized drift vector  $\mathbf{c}^0(\mathbf{Y}^0(t), t)$  can be expressed as

$$(4.7) \quad \mathbf{c}^0(\mathbf{Y}^0(t), t) = \mathbf{c}(\mathbf{Y}^0(t), t) - \mathbb{E}[\mathbf{c}(\mathbf{Y}^0(t), t)],$$

where the components of the centralized vector are given by

$$\begin{aligned}
c_1^0(\mathbf{Y}^0(t)) &= Y_2^0(t), \\
c_2^0(\mathbf{Y}^0(t)) &= -C_r(\tau)Y_2^0(t) - K_r(\tau)Y_1^0(t) - \frac{c^2\lambda_r^2}{2} \left( \frac{\Psi_L - 1}{L(\tau)} \right)^2 Y_1^0(t)\mu_{v_0}^2 \\
&\quad - \frac{c^2\lambda_r^2}{2} \left( \frac{\Psi_L - 1}{L(\tau)} \right)^2 ((Y_5^0(t))^2 Y_1^0(t) - \mathbb{E}[(Y_5^0(t))^2 Y_1^0(t)]) \\
&\quad + (Y_5^0(t))^2 \mu_{q_r} - \mathbb{E}[(Y_5^0(t))^2] \mu_{q_r} \\
&\quad - \frac{c^2\lambda_r^2}{2} \left( \frac{\Psi_L - 1}{L(\tau)} \right)^2 2(Y_5^0(t) Y_1^0(t) \mu_{v_0} - \mathbb{E}[Y_5^0(t) Y_1^0(t)] \mu_{v_0}) \\
&\quad + Y_5^0(t) \mu_{v_0} \mu_{q_r} \\
(4.8) \quad &\quad - \frac{c^2\lambda_r^2}{L(\tau)} (Y_3^0(t) Y_1^0(t) - \mathbb{E}[Y_3^0(t) Y_1^0(t)] + Y_1^0(t) \mu_{u_M}) + Y_3^0(t) \mu_{q_r} \\
&\quad - \frac{c^2\lambda_r^4}{4} (\tau) ((Y_1^0(t))^3 + 3(Y_1^0(t))^2 \mu_{q_r} - 3\mathbb{E}[(Y_1^0(t))^2] \mu_{q_r} + 3Y_1^0(t) \mu_{q_r}^2) \\
&\quad + (\beta_r^{(0)} - \beta_r^{(2)} \Omega_0^2) Y_5^0(t) + (\beta_r^{(1)} - 2\beta_r^{(2)} \zeta_f \Omega_0) Y_6^0(t) + \beta_r^{(2)} Y_7^0(t), \\
c_3^0(\mathbf{Y}^0(t)) &= Y_4^0(t), \\
c_4^0(\mathbf{Y}^0(t)) &= -\frac{EA}{M} \frac{\lambda_r^2(\tau)}{4} ((Y_1^0(t))^2 - \mathbb{E}[(Y_1^0(t))^2]) + 2Y_1^0(t) \mu_{q_r} - \omega_M^2(\tau) Y_3^0(t) \\
&\quad - 2\zeta_M \omega_M(\tau) Y_4^0(t) - \frac{EA}{2M} \left( \frac{\Psi_L - 1}{L(\tau)} \right)^2 ((Y_5^0(t))^2 \\
&\quad - \mathbb{E}[(Y_5^0(t))^2]) + 2Y_5^0(t) \mu_{v_0}), \\
c_5^0(\mathbf{Y}^0(t)) &= Y_6^0(t), \\
c_6^0(\mathbf{Y}^0(t)) &= -\Omega_0^2 Y_5^0(t) - 2\zeta_f \Omega_0 Y_6^0(t) + Y_7^0(t), \\
c_7^0(\mathbf{Y}^0(t)) &= -\alpha Y_7^0(t).
\end{aligned}$$

The diffusion vector is constant and is given as

$$(4.9) \quad \mathbf{d} = [0 \ 0 \ 0 \ 0 \ 0 \ 0 \ \alpha\sqrt{2\pi S_0}].$$

Instead of the non-linear system given in Eqs. (4.6) the linear one governed by the expression

$$(4.10) \quad d\mathbf{Y}^0(t) = \mathbf{B}\mathbf{Y}^0(t)dt + \mathbf{d}dW(t),$$

is considered with the centralized drift terms assumed as a linear form of the state variables

$$(4.11) \quad c_{i,eq}^0(\mathbf{Y}^0(t)) = B_{im} Y_m^0,$$

where coefficients  $B_{im}$  satisfy the following equations

$$(4.12) \quad B_{im}\kappa_{mj} = \mathbb{E}[Y_j^0 c_i^0(\mathbf{Y}^0)].$$

Equation (4.12) expressed in the matrix form is given as

$$(4.13) \quad \mathbf{B}\kappa(t) = \mathbb{E}[\mathbf{c}^0(\mathbf{Y}^0(t))\mathbf{Y}^{0T}].$$

Because the state variables  $\mathbf{Y}^0(t)$  are assumed to be the jointly Gaussian distributed, the relationship for a zero-mean Gaussian random vector  $\mathbf{X}$  given by ATALIK and UTKU [26] is used

$$(4.14) \quad \mathbb{E}[\mathbf{X}f(\mathbf{X})] = \mathbb{E}[\mathbf{X}\mathbf{X}^T]\mathbb{E}[\nabla f(\mathbf{X})],$$

with  $f(\mathbf{X})$  being non-linear function and  $\nabla = [\frac{\partial}{\partial X_1}, \frac{\partial}{\partial X_2}, \dots, \frac{\partial}{\partial X_n}]^T$ . Transposing both sides of Eq. (4.13) gives

$$(4.15) \quad \kappa^T(t)\mathbf{B}^T = \kappa(t)\mathbf{B}^T = \mathbb{E}[\mathbf{Y}^0\mathbf{c}^{0T}(\mathbf{Y}^0(t))].$$

Substituting expression presented in Eq.(4.14) into Eq.(4.15) yields

$$(4.16) \quad \kappa(t)\mathbf{B}^T = \kappa(t)\mathbb{E}[\nabla\mathbf{c}^{0T}(\mathbf{Y}^0(t))],$$

therefore the equivalent coefficients are obtained as

$$(4.17) \quad \mathbf{B}^T = \mathbb{E}[\nabla\mathbf{c}^{0T}(\mathbf{Y}^0(t))].$$

The matrix  $\mathbf{B}$  is obtained in the simplified form as

$$\mathbf{B} = \begin{bmatrix} 0 & 1 & 0 & 0 & 0 & 0 & 0 & 0 \\ -K_r(\tau) + D_r & -C_r(\tau) & -\frac{c^2\lambda_r^2}{L(\tau)}\mu_{qr} & 0 & F_r & \beta_r^{(1)} - 2\beta_r^{(2)}\zeta_f\Omega_0 & \beta_r^{(2)} & 0 \\ 0 & 0 & 0 & 1 & 0 & 0 & 0 & 0 \\ -\frac{EA\lambda_r^2(\tau)}{2M}\mu_{qr} & 0 & -\omega_M^2(\tau) & -2\zeta_M\omega_M(\tau) & -\frac{EA}{M}\left(\frac{\Psi_L-1}{L(\tau)}\right)^2\mu_{v_0} & 0 & 0 & 0 \\ 0 & 0 & 0 & 0 & 0 & 1 & 0 & 0 \\ 0 & 0 & 0 & 0 & -\Omega_0^2 & -2\zeta_f\Omega_0 & 1 & 0 \\ 0 & 0 & 0 & 0 & 0 & 0 & 0 & -\alpha \end{bmatrix},$$

where

$$(4.18) \quad \begin{aligned} K_r(\tau) &= \lambda_r^2 \left\{ \bar{c}^2 - V^2 + \frac{L(\tau)}{2}(a-g) \right\}, \\ C_r(\tau) &= 2\zeta_r\omega_r(\tau), \\ D_r &= -\frac{c^2\lambda_r^2}{L(\tau)}\mu_{u_M} - \frac{3c^2\lambda_r^4}{4}(\tau)(\mathbb{E}[(Y_1^0(t))^2] + \mu_{qr}^2) \\ &\quad - \frac{c^2\lambda_r^2}{2}\left(\frac{\Psi_L-1}{L(\tau)}\right)^2(\mathbb{E}[(Y_5^0(t))^2] + \mu_{v_0}^2), \\ F_r &= -c^2\lambda_r^2\left(\frac{\Psi_L-1}{L(\tau)}\right)^2(\mathbb{E}[Y_5^0(t)Y_1^0(t)] + \mu_{v_0}\mu_{qr}) + \beta_r^{(0)} - \beta_r^{(2)}\Omega_0^2. \end{aligned}$$

The covariance matrix  $\mathbf{R}_{\mathbf{Y}^0\mathbf{Y}^0} = E[\mathbf{Y}^0\mathbf{Y}^{0T}]$  is governed by the equations

$$(4.19) \quad \frac{d}{dt}\mathbf{R}_{\mathbf{Y}^0\mathbf{Y}^0} = \mathbf{B}\mathbf{R}_{\mathbf{Y}^0\mathbf{Y}^0} + \mathbf{R}_{\mathbf{Y}^0\mathbf{Y}^0}\mathbf{B}^T + \mathbf{d}\mathbf{d}^T,$$

which should be solved together with differential equations for mean values Eq. (4.3).

## 5. Numerical results

In the analysis, the case of the elevator's motion downwards, from the top level to the ground level is considered. In the computation the height of the entire system is given as  $Z_0 = 243.5$  m and the initial length of the cable  $L(0) = 7.5$  m has been assumed. The mass of the lift car is assumed as  $M = 500$  kg while the properties of the cable such as mass per unit length as  $m = 1.3$  kg/m and tensile stiffness as  $EA = 15.1$  MN. The host structure is subjected to the fundamental resonance sway with the frequency  $\Omega_0 = 0.25$  Hz and the amplitude at the top level given as  $A_0 = 0.3$  m. Because the length of the cable increases over time the undamped frequency of the first mode  $\omega_1$  varies slowly over time in the range from 4 HZ to 0.17 Hz. It reaches the value of 0.25 HZ for  $L$  that is approximately 132.9 m which corresponds to the time instant 37.5 s (see Fig. 2). Simultaneously the undamped longitudinal frequency of the mass vibration also varies slowly over time from 10.9 Hz to the 1.9 Hz, however its value is several times larger in comparison with the  $\omega_1$ .

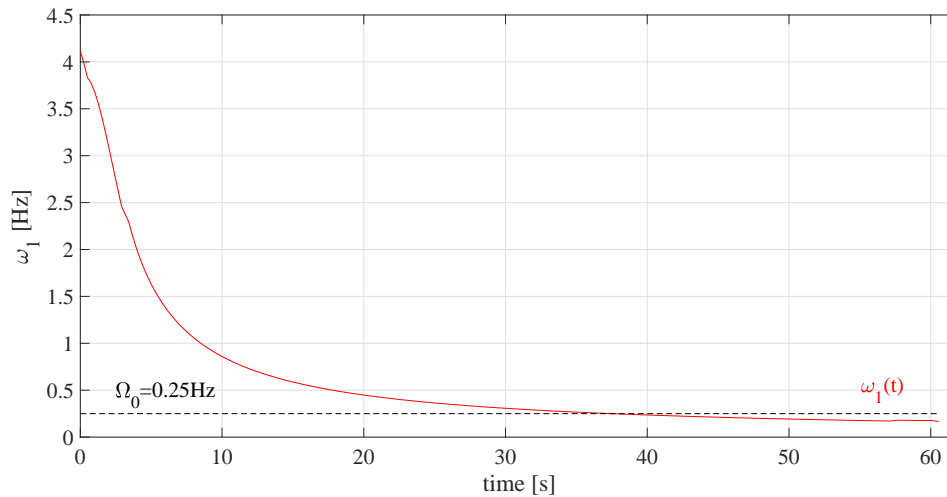


FIG. 2. Variation of the system natural frequency.

The deterministic values of generalized coordinates and the longitudinal vibrations of the mass were obtained from the non-linear system using  $r = 1$ , the damping ratios  $\zeta_r = \zeta_M = 0.03$  and transport speed  $V = 3.5$  m/s. The stochastic analysis of the linear system given by the differential equations (4.3) and (4.19) has been conducted for different values of the damping ratio of the auxiliary filter  $\zeta_f$ . The comparison of deterministic results of generalized coordinates and vertical displacements of the concentrated mass with their expected values obtained by equivalent linearization technique is presented in Fig. 3(a, b).

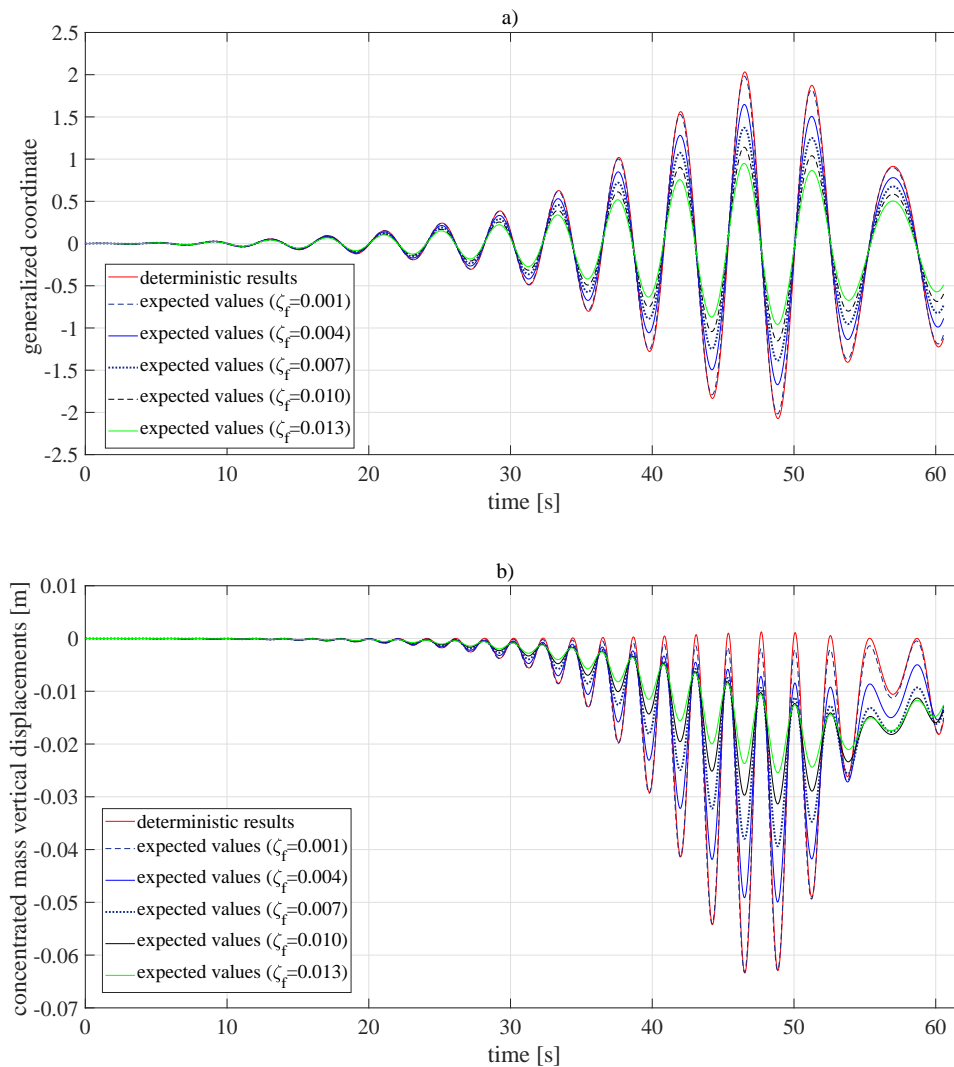


FIG. 3. Comparison of deterministic results and expected values obtained by the equivalent linearization technique.

The plots show, that the smaller the value of the  $\zeta_f$  the better match between the stochastic and deterministic results can be observed. This is so, because the smaller the value  $\zeta_f$  the smaller the bandwidth of the narrow-band stochastic process  $v_0(t)$ , hence the narrow-band process approaches, in some sense, the harmonic process. Both deterministic and stochastic values of  $q_r$  and  $u_M$  show a significant increase of their values after entering the system into the resonance area. The deterministic and the stochastic responses have compatible phases and tend to decrease after reaching their maximum values. The difference between the results obtained for the deterministic harmonic excitation and for mean-square equivalent narrow-band stochastic excitation may be explained by the fact that the deterministic response is the response of the original non-linear system, whereas the response to the narrow-band stochastic excitation is the response of a linearized system.

The diagrams of the variances of the particular random state variables over time are shown in Fig. 4. For  $\text{Var}[q_r]$ ,  $\text{Var}[v_0]$  and  $\text{Var}[X]$  increasing the value of the damping ratio  $\zeta_f$  results in larger values of variance. However, the behaviour of the  $\text{Var}[u_M]$  diagram is opposite – the bigger the damping filter ratio the lower the value of variance. On the other hand, results of  $\text{Var}[u_M]$  are significantly lower in comparison with the variances of other variables, and for very small  $\zeta_f$  below 0.004 can give false results (compare Fig. 4b). For the assumed amplitude of the sway  $A_0 = 0.3$  m, the condition given by Eq. (3.3) yields 0.045. Figure 4c shows that for  $\zeta_f$  equal 0.01 and higher the  $\text{Var}[v_0]$  tends to 0.045, so the requirement is satisfied.

For additional verification the values of random state variables obtained by the equivalent linearization technique are compared with results obtained by the Monte Carlo simulation, which is numerically approximate method and its accuracy depends on the step of the integration as well as on the number of tests used during the analysis. Hence there may be some differences in results between both methods. Monte Carlo simulation was first conducted by using 1000 simulation tests (see Figs. 5 and 6), for three different time steps:  $\Delta t = (0.03; 0.05; 0.1)$  [s] and for the coefficient  $\zeta_f = 0.01$ , which gives acceptable results for all random variables in an equivalent linearization technique. In next step the comparison for the coefficient  $\zeta_f = 0.001$  was made, for which the best matches between the deterministic and stochastic results are reached. In the second case the Monte Carlo simulation was conducted by using 1500 simulation tests for one time step  $\Delta t = 0.03$  s (see Figs. 7 and 8).

Verification of results obtained for  $\zeta_f = 0.01$  from equivalent linearization against Monte Carlo simulations shows a very good accuracy of the predicted mean value  $E[q_r]$  (Fig. 5a). The prediction of the mean value  $E[u_M]$  (Fig. 5b) and of the variances  $\text{Var}[q_r]$ ,  $\text{Var}[u_M]$  (Fig. 6a, b) is less accurate. Very good agreement between the results obtained from equivalent linearization and those

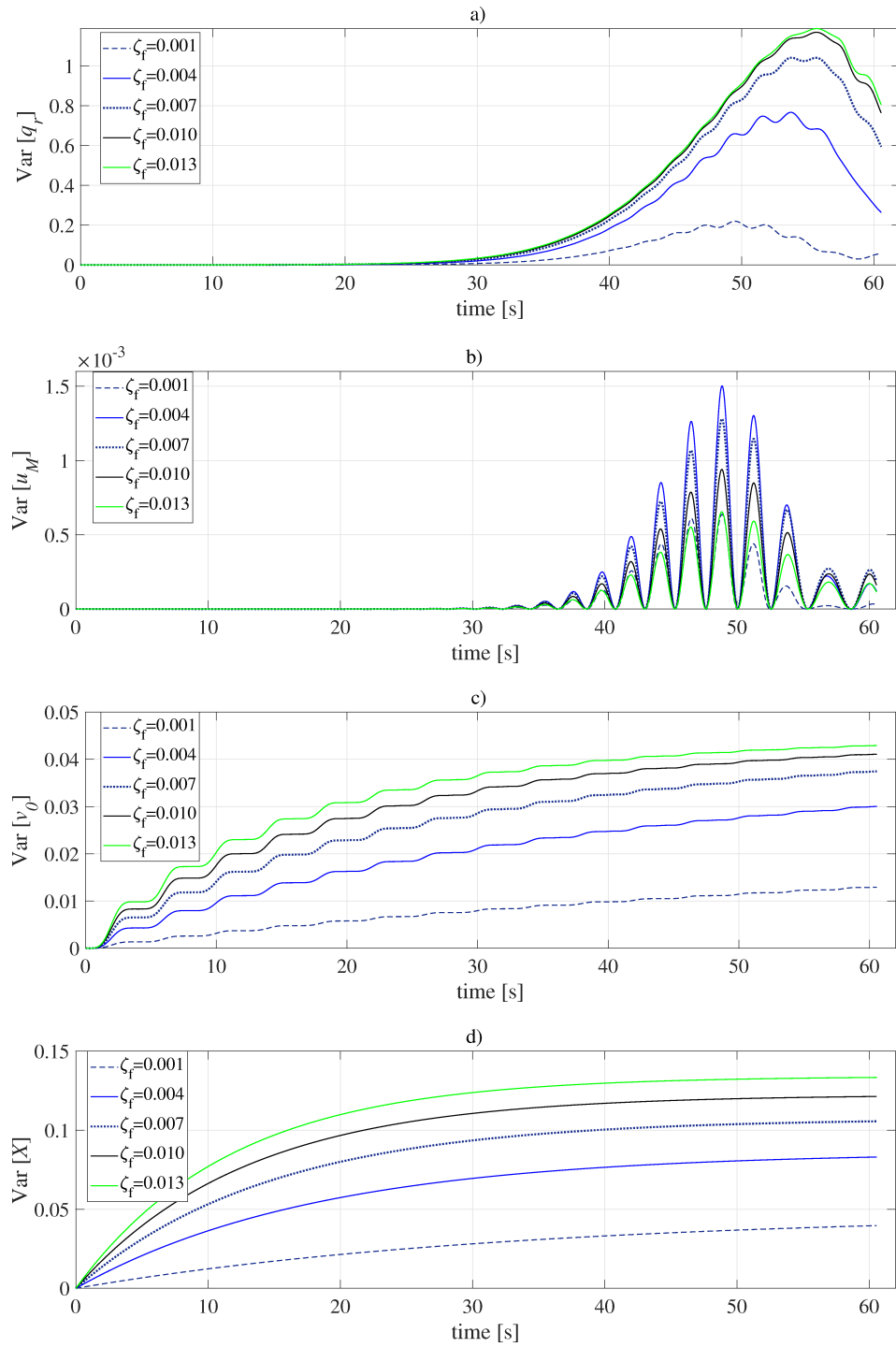


FIG. 4. Variances of particular random state variables obtained by equivalent linearization.

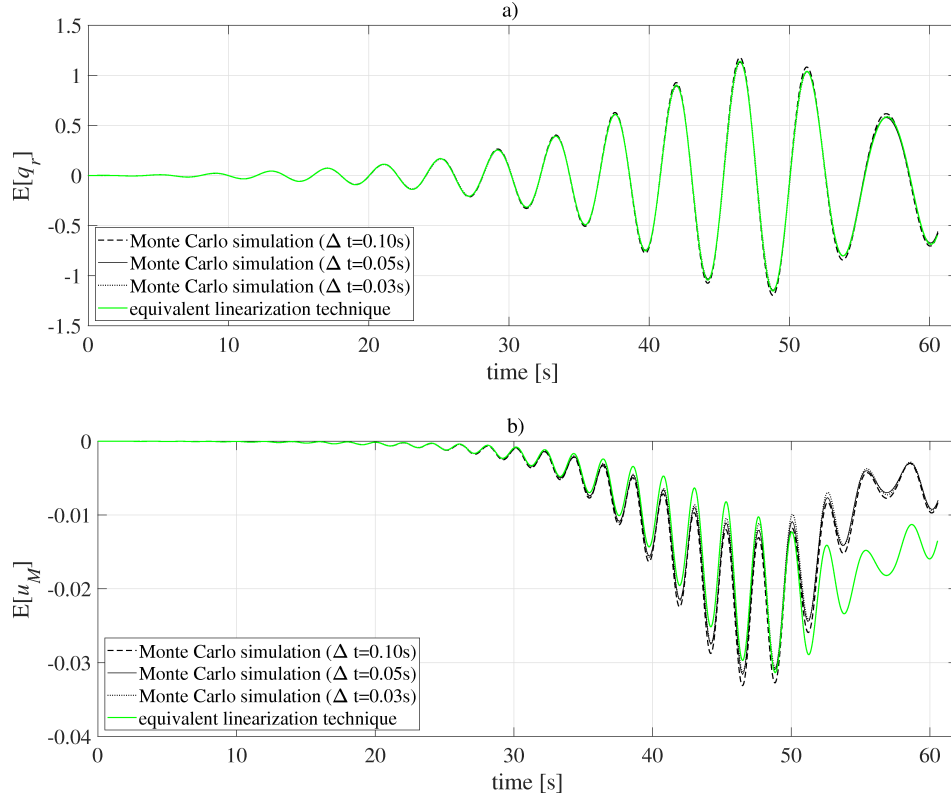


FIG. 5. Comparison of expected values obtained for  $\zeta_f = 0.01$ .

from Monte Carlo simulations in the case of  $\text{Var}[v_0]$  and  $\text{Var}[X]$  (Fig. 6c,d) may be explained by the fact that the processes  $v_0(t)$  and  $X(t)$  are governed by linear equations (3.1), appended to the non-linear system. As the result of equivalent linearization technique the statistics for the generalized coordinate  $q_r$  and for the vertical mass displacement  $u_M$  are only approximate. However, as  $v_0(t)$  and  $X(t)$  are governed by autonomous linear equations (3.1), their statistics are exact. Indeed, the coefficients in the equivalent matrix  $\mathbf{B}$ , given by (4.18), corresponding to the variables  $v_0(t)$ ,  $\dot{v}_0(t)$  and  $X(t)$ , i.e. the bottom-right ( $3 \times 3$ ) sub-block  $\mathbf{B}_{22}$  of the matrix  $\mathbf{B}$  are the exact coefficients of the linear system (auxiliary filters) governed by (3.1)

$$(5.1) \quad \mathbf{B}_{22} = \begin{bmatrix} 0 & 1 & 0 \\ -\Omega_0^2 & -2\zeta_f\Omega_0 & 1 \\ 0 & 0 & -\alpha \end{bmatrix}.$$

If in Eq. (4.19) the matrices are subdivided into pertinent sub-blocks and the

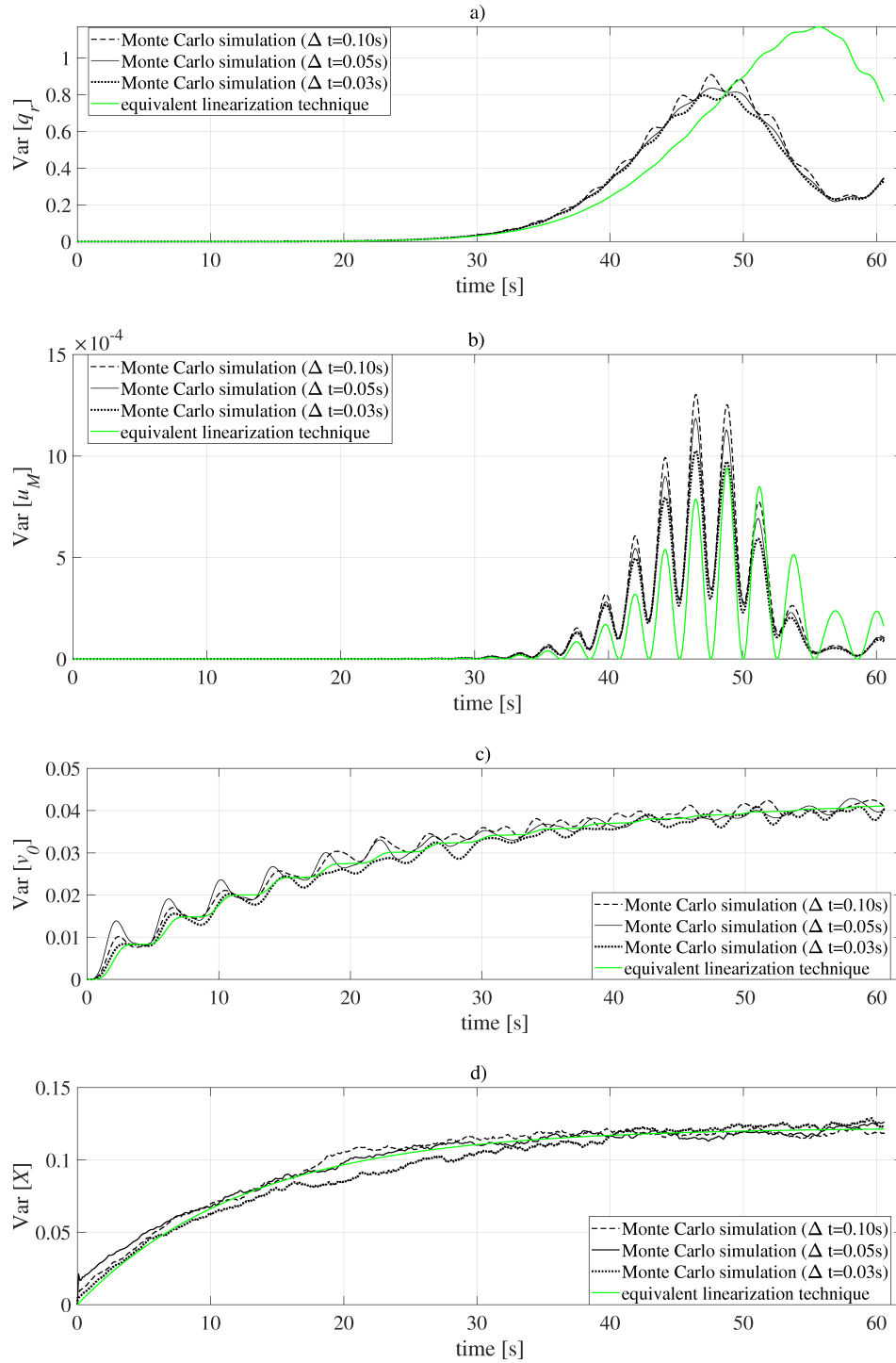


FIG. 6. Comparison of particular random state variables obtained for  $\zeta_f = 0.01$ .

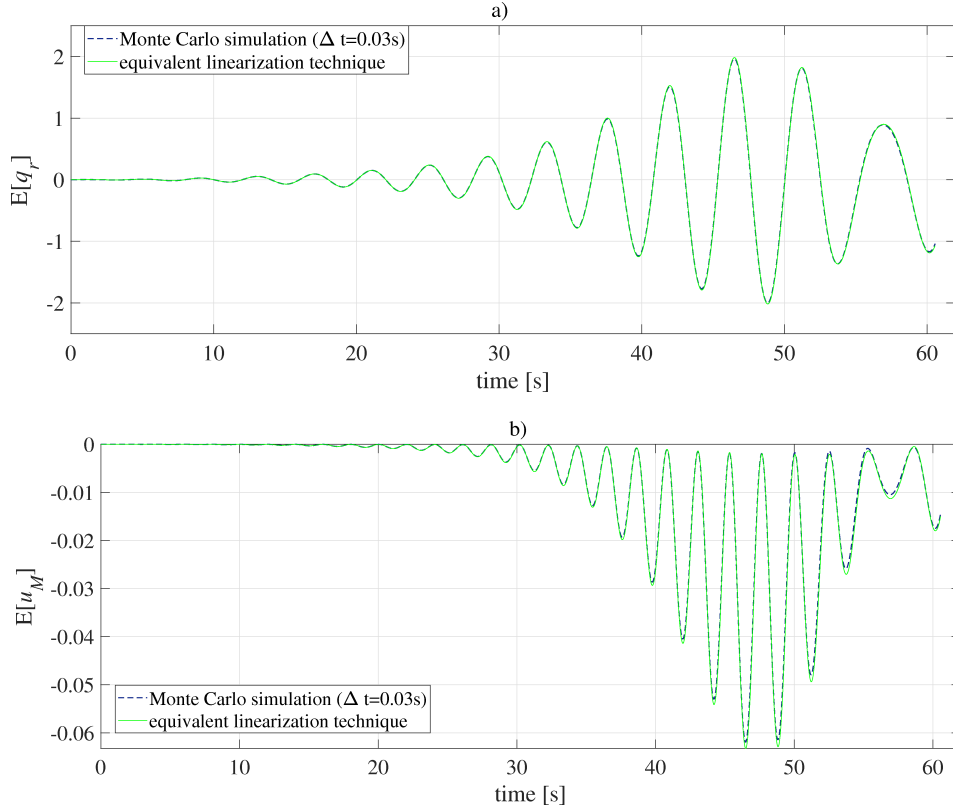


FIG. 7. Comparison of expected values obtained for  $\zeta_f = 0.001$ .

multiplication of sub-matrices is carried out, the equation governing the covariance matrix  $\mathbf{R}_{22}(t)$  of the state variables  $v_0(t)$ ,  $\dot{v}_0(t)$  and  $X(t)$ , which is the bottom-right  $(3 \times 3)$  sub-block of the matrix  $\mathbf{R}_{\mathbf{Y}_0\mathbf{Y}_0}$  is obtained as

$$(5.2) \quad \frac{d}{dt} \mathbf{R}_{22}(t) = \mathbf{B}_{22} \mathbf{R}_{22} + \mathbf{R}_{22} \mathbf{B}_{22}^T + \begin{bmatrix} 0 & 0 & 0 \\ 0 & 0 & 0 \\ 0 & 0 & 2\pi S_0 \alpha^2 \end{bmatrix}.$$

This equation is independent of the equations for cross-covariances of other state variables and represents the exact equation governing the cross-covariances of the state variables of the linear system (auxiliary filters) governed by (3.1). Hence the variances  $\text{Var}[v_0]$  and  $\text{Var}[X]$  obtained from equivalent linearization are exact.

Comparison of the results obtained by two mentioned methods for the coefficient  $\zeta_f = 0.001$  shows a very good match between the diagrams for the expected values of  $q_r$  and  $u_M$  (see Fig. 7). The prediction of the variances of the generalized coordinate  $q_r$  and of the longitudinal displacement  $u_M$  of the mass obtained

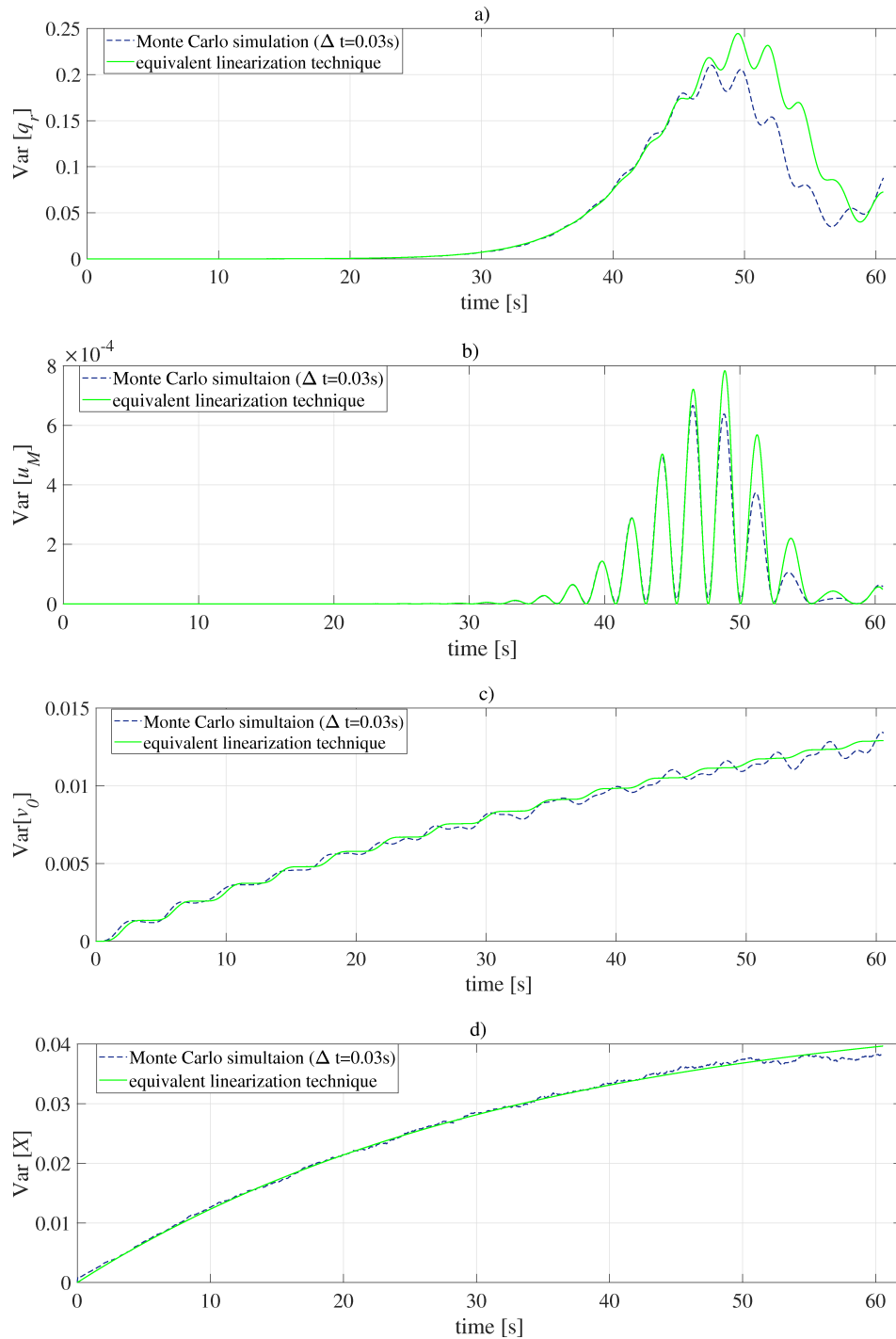


FIG. 8. Comparison of particular random state variables obtained for  $\zeta_f = 0.001$ .

from the equivalent linearization technique (Figs. 8a, b) is more accurate than for  $\zeta_f = 0.01$ . As explained before, the variances of  $v_0(t)$  and  $X(t)$  obtained from the equivalent linearization technique are exact. The fluctuations observed in pertinent plots (Figs. 6c, d and 8c, d) obtained by Monte Carlo simulations are of numerical nature.

Comparing the graphs the following regularity can be observed – as time increases the accuracy of approximate results obtained from equivalent linearization decreases (Fig. 5b, Figs. 6a, b and Figs. 8a, b). The time evolution of the response of the linearized system is different from the time evolution of the original non-linear system. These two responses differ quantitatively that can be especially seen in the resonance region. However, qualitative behaviour appears to be similar. That brings about a conclusion that for significant values of the damping ratio of an auxiliary filter the accuracy of the equivalent linearization technique is limited to the initial resonance stage. Unfortunately the methods of estimation of the error associated with the equivalent linearization technique are not known. Therefore the results are verified against Monte Carlo simulations.

The expected value of longitudinal displacement of the concentrated mass and its variance, as well as the variance of generalized coordinate become very sensitive to the variation of the value  $E[X]$  in numerical analysis. As the expected value of the white noise  $E[\xi(t)] = 0$ , from the linear model (3.1) it follows that  $E[X(t)] = 0$  at every time instant. However, the simulation of white noise excitation by using random data and including it in the numerical solution by using the Monte Carlo technique yields small deviation of  $E[X]$  from 0 at some time points. The results in fluctuating behaviour of simulated results for variances of  $v_0(t)$  and  $X(t)$  observed in Figs. 6a, b and Figs. 8a, b, especially in the former ones. It would also be worth to note that the computational time involved in the equivalent linearization technique is several times shorter in comparison with the Monte Carlo simulation.

## 6. Concluding remarks

The study conducted and reported in this paper concerns a cable-mass system with time-varying length. The proposed model can be applied in the design considerations of high-rise buildings with modular installations such as passenger lifts/elevators that are exposed to dynamic external loads. The mathematical model presented in this work accounts for the non-linear effects of cable stretching and is used to determine the response of the system to the base-motion excitation caused by low-frequency sway of the host structure. A single-mode approximation is employed for the lateral response of the system. The stochastic excitation assumed as a narrow-band random process mean-square equivalent to a deterministic harmonic process is idealized as the output of a system of two

auxiliary linear filters to the input in the form of a Gaussian white noise process. An equivalent linearization technique is then used to determine the stochastic response of the system. The equations for mean values and the covariance matrix of the state variables are solved numerically. The mean value and variance of the transverse displacement of the cable and of the longitudinal motion of the lumped mass, as well as deterministic results obtained for a harmonic excitation, are presented. The mean behaviour of the stochastic response is similar to the behaviour of the deterministic response, especially for lower values of the filter damping ratio, i.e. when the bandwidth of the random process is small. Prediction of the variances of the response variables by the equivalent linearization technique is sufficiently accurate, especially for low values of the auxiliary filter damping ratio (hence for a small bandwidth of the narrow-band process  $v_0(t)$ ) and in the initial phase of the resonance. The simulation results show the effectiveness of the application of the equivalent linearization technique to the non-linear problem involved.

A comparison of the results obtained by the application of the equivalent linearization technique with those determined from the non-linear deterministic model, as well as with the results obtained from the Monte Carlo method, leads to the conclusion that the proposed linearization technique can be successfully applied in the analysis of random behaviour of traction-drive vertical transportation systems. The results demonstrate that the equivalent linearization technique is effective in reducing the computational times required to predict the response of the system without compromising the accuracy. It can be concluded that if appropriately tuned stochastic characteristics are selected in the stochastic analysis the results are comparable with the dynamic response levels that are determined by using other established methods such as the Monte Carlo simulation technique.

## References

1. J.P. ANDREW, S. KACZMARCZYK, *Systems Engineering of Elevators*, Elevator World, Mobile, Alabama, 2011.
2. M.P. CARTMELL, D.J. MCKENZIE, *A review of space tether research*, Progress in Aerospace Sciences, **44**, 1–21, 2008.
3. R.M. EVAN-IWANOWSKI, *Resonance Oscillations in Mechanical Systems*, Elsevier Scientific Publishing Company, Amsterdam, 1976.
4. N.J. COOK, *The Designer's Guide to Wind Loading of Building Structures Part 1*, Butterworths, London, 1985.
5. T. KJIEWSKI-CORREA, D. PIRINIA, *Dynamic behavior of tall buildings under wind: insights from full-scale monitoring*, The Structural Design of Tall Special Buildings, **16**, 471–486, 2007.

6. G.R. STRAKOSCH, *The Vertical Transportation Handbook*, John Wiley, New York, 1998.
7. J.W. LARSEN, R. IWANKIEWICZ, S.R.K. NIELSEN, *Probabilistic stochastic stability analysis of wind turbine wings by Monte Carlo simulations*, Probabilistic Engineering Mechanics, **22**, 181–193, 2007.
8. S. KACZMARCZYK, R. IWANKIEWICZ, *Gaussian and non-Gaussian stochastic response of slender continua with time-varying length deployed in tall structures*, International Journal of Mechanical Sciences, **134**, 500–510, 2017.
9. G.F. GIACCU, B. BARBIELLINI, L. CARACOGLIA, *Stochastic unilateral free vibration of an in-plane cable network*, Journal of Sound and Vibration, **340**, 95–111, 2015.
10. S. KACZMARCZYK, R. IWANKIEWICZ, Y. TERUMICHI, *The dynamic behaviour of a non-stationary elevator compensating rope system under harmonic and stochastic excitations*, Journal of Physics: Conference Series, **181**, 012–047, 2009.
11. Y. TERUMICHI, M. OHTSUKA, M. YOSHIKAWA, Y. FUKAWA, Y. TSUJIOKA, *Nonstationary vibrations of a string with time-varying length and a mass-spring system attached at the lower end*, Nonlinear Dynamics, **12**, 39–55, 1995.
12. Y.A. MITROPOLSKII, *Problems of the Asymptotic Theory of Nonstationary Vibrations*, Israel Program for Scientific Translations Ltd, Jerusalem, 1965.
13. S. KACZMARCZYK, R. IWANKIEWICZ, *On the nonlinear deterministic and stochastic dynamics of a cable – mass system with time-varying length*, 12th International Conference on Structural Safety and Reliability, Austria, 1205–1213, 2017.
14. T.K. CAUGHEY, *Equivalent linearization techniques*, The Journal of the Acoustical Society of America, **35**, 1706–1711, 1963.
15. J.B. ROBERTS, *Response of non-linear mechanical systems to random excitations: Part II: Equivalent linearization and other methods*, Shock and Vibration Digest, **13**, 5, 15–29, 1981.
16. P.D. SPANOS, *Stochastic linearization in structural dynamics*, Applied Mechanics Reviews, A.S.M.E., **34**, 1–8, 1981.
17. J.B. ROBERTS, P.D. SPANOS, *Random Vibration and Statistical Linearization*, Wiley, Chichester, New York, 1990.
18. L. SOCHA, *Linearization Methods for Stochastic Dynamic systems*, Lecture Notes in Physics 730, Springer, Heidelberg, 2008.
19. A. TYLIKOWSKI, W. MAROWSKI, *Vibration of a non-linear single-degree-of-freedom system due to Poissonian impulse excitation*, International Journal of Non-Linear Mechanics, **21**, 229–238, 1986.
20. M. GRIGORIU, *Response of dynamic systems to Poisson white noise*, Journal of Sound and Vibration, **195**, 3, 375–389, 1996.
21. R. IWANKIEWICZ, S.R.K. NIELSEN, *Dynamic response of hysteretic systems to Poisson-distributed pulse trains*, Probabilistic Engineering Mechanics, **7**, 135–148, 1992.
22. P.D. SPANOS, G.I. EVANGELATOS, *Response of nonlinear system with restoring forces governed by fractional derivatives – time domain simulation and statistical linearization solution*, Soil Dynamics and Earthquake Engineering, **30**, 811–821, 2010.

23. P.D. SPANOS, I.A. KOUGIOUMTZOGLOU, *Harmonic wavelets based statistical linearization for response evolutionary power spectrum determination*, Probabilistic Engineering Mechanics, **27**, 57–68, 2012.
24. F. KONG, P.D. SPANOS, J. LI, I.A. KOUGIOUMTZOGLOU, *Response evolutionary power spectrum determination of chain-like MDOF non-linear structural systems via harmonic wavelets*, International Journal of Non-Linear Mechanics, **66**, 3–17, 2014.
25. I.A. KOUGIOUMTZOGLOU, V.C. FRAGKOULIS, A.A. PANTELOUS, A. PIRROTTA, *Random vibration of linear and nonlinear structural systems with singular matrices: a frequency domain approach*, Journal of Sound and Vibration, **404**, 84–101, 2017.
26. T.S. ATALIK, S. UTKU, *Stochastic linearization of multi-degree-of-freedom nonlinear systems*, Earthquake Engineering Structures Dynamics, **4**, 411–420, 1976.

Received November 30, 2018; revised version August 25, 2019.

Published online October 25, 2019.

---